ARTICLE
Journal of Cellular Biochemistry 112:829–839 (2011)

Journal of Cellular Biochemistry

Essential Roles of the Nitric Oxide (NO)/cGMP/Protein Kinase G type-Iα (PKG-Iα) Signaling Pathway and the Atrial Natriuretic Peptide (ANP)/cGMP/PKG-Iα Autocrine Loop in Promoting Proliferation and Cell Survival of OP9 Bone Marrow Stromal Cells

Janica C. Wong[1,2] and Ronald R. Fiscus[1,2,3*]

[1]*Cancer Molecular Biology Section, Nevada Cancer Institute, Las Vegas, Nevada 89135*

[2]*Department of Chemistry, University of Nevada Las Vegas, Las Vegas, Nevada 89154*

[3]*College of Pharmacy, University of Southern Nevada, Henderson, Nevada 89014*

ABSTRACT

Inappropriate signaling conditions within bone marrow stromal cells (BMSCs) can lead to loss of BMSC survival, contributing to the loss of a proper micro-environmental niche for hematopoietic stem cells (HSCs), ultimately causing bone marrow failure. In the present study, we investigated the novel role of endogenous atrial natriuretic peptide (ANP) and the nitric oxide (NO)/cGMP/protein kinase G type-Iα (PKG-Iα) signaling pathway in regulating BMSC survival and proliferation, using the OP9 BMSC cell line commonly used for facilitating the differentiation of HSCs. Using an ANP-receptor blocker, endogenously produced ANP was found to promote cell proliferation and prevent apoptosis. NO donor SNAP (S-nitroso-*N*-acetylpenicillamine) at low concentrations (10 and 50 μM), which would moderately stimulate PKG activity, protected these BMSCs against spontaneous apoptosis. YC-1, a soluble guanylyl cyclase (sGC) activator, decreased the levels of apoptosis, similar to the cytoprotective effects of low-level NO. ODQ (1H-[1,2,4]oxadiazolo[4,3,-a]quinoxalin-1-one), which blocks endogenous NO-induced activation of sGC and thus lowers endogenous cGMP/PKG activity, significantly elevated apoptotic levels by 2.5- and three-fold. Pre-incubation with 8-Bromo-cGMP or ANP, which bypass the ODQ block, almost completely prevented the ODQ-induced apoptosis. A highly-specific PKG inhibitor, DT-3, at 20, and 30 μM, caused 1.5- and two-fold increases in apoptosis, respectively. ODQ and DT-3 also decreased BMSCs proliferation and colony formation. Small Interfering RNA gene knockdown of PKG-Iα increased apoptosis and decreased proliferation in BMSCs. The data suggest that basal NO/cGMP/PKG-Iα activity and autocrine ANP/cGMP/PKG-Iα are necessary for preserving OP9 cell survival and promoting cell proliferation and migration. J. Cell. Biochem. 112: 829–839, 2011.

KEY WORDS: PROTEIN KINASE G; BONE MARROW STROMAL CELLS; PROLIFERATION; APOPTOSIS

Bone marrow stromal cells (BMSCs) have been implicated in a wide range of clinical applications and regenerative medicine, such as tissue repair [Kitada and Dezawa, 2009], myocardial infarction [Psaltis et al., 2008] and neurodegenerative diseases [Sadan et al., 2009]. BMSCs were first characterized by Friedenstein et al. [1968] as an adherent, fibroblast-like population in the adult bone marrow. Multipotent BMSCs are capable of differentiating along the mesenchymal lineage to form bone, fat, and cartilage [Caplan, 1991; Hassan and El-Sheemy, 2004] and potentially could be used to regenerate other tissues. Also, BMSCs provide a proper micro-environmental niche for the growth/cultivation of hematopoietic stem cells (HSCs) [Wilson and Trumpp, 2006]. The proper environment for HSCs in the bone marrow requires several specific groups of cells, including endothelial cells and BMSCs and, along with the extracellular matrix elements, interact with HSCs to promote/inhibit their self renewal, differentiation and migration.

Our early studies had identified cGMP-dependent protein kinase (protein kinase G, PKG) as a key protein kinase mediating the vasodilatory effects of nitric oxide (NO) and atrial natriuretic peptide (ANP, ANF, atriopeptin) in blood vessels, specifically by relaxing the vascular smooth muscle cells (VSMCs) within the walls

Grant sponsor: The US Department of Defense; Grant number: W81XWH-07-1-0543.

*Correspondence to: Ronald R. Fiscus, College of Pharmacy, University of Southern Nevada, 11 Sunset Way, Henderson, NV 89014. E-mail: rfiscus@usn.edu

Received 12 August 2010; Accepted 22 November 2010 • DOI 10.1002/jcb.22981 • © 2010 Wiley-Liss, Inc.
Published online 28 December 2010 in Wiley Online Library (wileyonlinelibrary.com).

of these vessels [Fiscus et al., 1983, 1985; Fiscus, 1988; Fiscus and Murad, 1988]. More recent studies from our laboratory have shown that basal or moderately elevated PKG activity is essential for the survival of certain neural cell lines, including PC12, N1E-115 and NG108-15 cells [Fiscus et al., 2001, 2002; Fiscus, 2002; Cheng Chew et al., 2003; Johlfs and Fiscus, 2010]. Our laboratory has also shown that basal PKG activity plays a similar cytoprotective role in preventing spontaneous apoptosis in primary murine VSMCs, immortalized uterine epithelial cells, and human ovarian cancer cells [Chan and Fiscus, 2003; Fraser et al., 2006; Leung et al., 2008, 2010; Wong and Fiscus, 2010].

Although research on stem cells has increased drastically in recent years, there are very few studies on the role of the NO/cGMP/PKG pathway in stem cells [Krumenacker et al., 2006]. Expression of mRNA and protein levels of the three NOSs and sGC has been reported in mouse embryonic stem (ES) cells and the expression of PKG in ES cell-derived cardiomyocytes is known to increase during differentiation [Krumenacker and Murad, 2006]. Very recently, the NO/cGMP/PKG signaling pathway has been proposed to promote stem cell-like characteristics in glioma cells in the tumor perivascular niche of medulloglioma [Charles et al., 2010].

In the present study, the BMSC cell line OP9 was used to investigate the role of endogenous ANP/cGMP/PKG and NO/cGMP/PKG signaling pathways in BMSCs. These cells are mouse BMSCs lacking the expression of macrophage-colony stimulating factor, making them especially useful as a feeder layer for hematopoietic differentiation down a lineage other than monocytes. OP9 cells are reported to augment the survival of hematopoietic precursors and progenitors [Ji et al., 2008], and can be used in a coculture system with mouse ES cells and induced pluripotent stem (iPS) cells to induce the differentiation of ES cells into endothelial cells [Kelly and Hirschi, 2009] and blood cells of erythroid, myeloid, and B cell lineages [Nakano et al., 1994; Nakano, 1995; Kitajima et al., 2003; Ji et al., 2008], and iPS into hematopoietic cell lineages [Niwa et al., 2009].

MATERIALS AND METHODS

CELL CULTURE AND TISSUE

OP9 mouse BMSCs were purchased from American Type Culture Collection (ATCC). BMSCs were cultured in α-Minimum Eagle's Medium (α MEM), supplemented with fetal bovine serum (20%),streptomycin (50 μg/ml), and penicillin (50 units/ml) (all from Lonza), and cultured at 37°C in an atmosphere of 5% CO_2/95% air.

The aortas were isolated from mice as previous described [Wong and Fiscus, 2010]. The mice were obtained from Jackson Laboratories. The treatment of laboratory animals and the experimental procedures of the present study adhered to the NIH Guidelines for Animal Care, and were approved by IACUC at the Nevada Cancer Institute.

PROTEIN EXTRACTION AND WESTERN BLOTTING USING INFRARED IMAGING

For protein extraction, the cells were lysed using 85°C hot 1× sodium dodecyl sulfate (SDS) lysis buffer (50 mmol/L Tris–HCL, pH 6.8, 2% SDS, 10 mmol/L dithiolthreitol, and 10% glycerol). The supernatant fractions were collected by centrifugation (15,000*g*; 10 min). The total amount of protein in the lysates was calculated from the fluorescence-based protein quantitation kit EZQ (Molecular Probes). Proteins were separated on 4–12% polyacrylamide NuPage gels (Invitrogen) and then transferred to nitrocellulose membranes. Membranes were blocked (room temperature, 1 h) with blocking buffer (Rockland Immunochemicals), then incubated at 4°C overnight with primary antibodies [PKG-Iα/β (1:1,000), p-(ser-239)-vasodilator-stimulated phosphoprotein (VASP; 1:500), total VASP (1:1,000), eNOS (1:1,000), p-(ser-1,177)-eNOS (1:1,000), total PARP (1:1,000), and cleaved PARP (1:1,000) (all from Cell Signaling Technology), KLF4 (1:1,000) (Chemicon), NPR-A (1:500), ANP (1:1,000), β-actin (1:1,000) (Santa Cruz Biotechnology)] and subsequently with secondary antibodies labeled with infrared dyes (LI-COR Biosciences) (1:25,000 in blocking buffer; room temperature for 1 h). The membranes were scanned on the Odyssey infrared imaging system (LI-COR Biosciences).

CLONOGENIC CELL SURVIVAL ASSAY

Clonogenic assays were used to assess the cell survival in cells after treatment with sGC inhibitor ODQ, sGC activator YC-1, and selective PKG-Iα inhibitor DT-3 (Calbiochem). Around 500 cells per well were plated in six-well plates, treated with ODQ (10, 40, and 100 μM), YC-1 (5, 10, 20, 40, and 100 μM) and DT-3 (10, 20 and 30 μM) for 24 h. After the incubation period the cells were washed with 1× PBS (Lonza) twice and once with fresh media. Fresh media was added and cells were incubated for 7–10 days to form colonies (or until control wells attain confluency), followed by staining with crystal violet (5 mg/ml crystal violet in 95% ethanol). The number of colonies in the controls and treatments were counted and compared. Acetic acid (10%) was used to dissolve the crystal violet, and the amount of color was quantified with a spectrophotometer at absorbance 570 nm.

ASSESSMENT OF CELL PROLIFERATION BY MTT ASSAY

Proliferation of BMSCs was measured by MTT assay (Roche Applied Science), following the protocol of the manufacturer.

ASSESSMENT OF DE NOVO DNA SYNTHESIS BY BrdU-(5′Bromo-2-deoxyuridine) ELISA COLORIMETRIC ASSAY

The rate of DNA synthesis of BMSCs was measured by BrdU ELISA assay (Roche Applied Science), following protocol of the manufacturer. Cells were seeded in 96-well microplates (1×10^3 cells per well) and incubated at 37°C in 5% CO_2 for 24 h, followed by treatment for 72 h with BrdU label.

ASSESSMENT OF APOPTOSIS BY CELL DEATH DETECTION ELISA PLUS

The Cell Death Detection ELISA^{PLUS} assay (Roche Applied Science), based on quantitative sandwich-enzyme-immunoassay-principle with monoclonal antibodies directed against DNA and histones, were used to quantify apoptotic levels in BMSCs treated with ODQ, SNAP, YC-1, and DT-3 (Calbiochem), 8-Br-cGMP (Sigma) and ANP (Phoenix Pharmaceuticals). Procedures followed the manufacturer's protocol, with the following exception. A longer centrifugation time (i.e., 30 min, instead of the recommended 10 min), after cell permeation for releasing apoptotic fragments of DNA, was used in

order to obtain a cleaner separation of apoptotic DNA fragments from genomic DNA in cell nuclei. This modification dramatically lowered background interference caused by contaminating genomic DNA and thus allowed better quantification of apoptotic responses.

MEASUREMENTS OF cGMP LEVELS BY ENZYME-LINKED-IMMUNOASSAY

Levels of cGMP were measured by an enzyme-linked immunoassay (Assay Designs) as described previously [Wong and Fiscus, 2010].

SMALL INTERFERING RNA (siRNA) GENE KNOCKDOWN

For siRNA-mediated silencing of gene expression, cells were transfected with 50 nmol/L and 100 nmol/L Stealth™ RNAi (siRNA, 5'-GAGGAAGACUUUGCCAAGAUUCUCA-3') for specifically targeting the expression of PKG-Iα (Invitrogen). Transfection of BMSCs was conducted using RNAiMAX (Invitrogen). Non-silencing siRNA (Invitrogen) was used as the negative control. At 72 h after transfection, the culture medium was changed and fresh medium was supplied. The cells were used in experiments 16 h later.

IN VITRO CELL MIGRATION (INVASION) ASSAY

Migration of cells was assessed using transwells (Corning) containing inserts with polycarbonated filter of 8 μM pore size. The inserts were coated with growth factor-reduced matrigel (BD Bioscience) at 37°C for 30 min. The upper chamber contained 4×10^4 cells in 0.1 ml complete medium mixed with inhibitors or DMSO (control). The lower chamber contained 0.6 ml of complete medium with the same concentration of the inhibitors or DMSO. Migration through the membrane was determined after 24 h of incubation at 37°C. Cells remaining on the topside of the transwell membrane were removed using a cotton swab. The membrane was washed with ice-cold PBS. Cells that had migrated to bottom side were stained with 0.5% crystal violet.

STATISTICAL ANALYSIS

Results are expressed as the mean ± standard error of at least four independent experiments. Statistical analysis was performed by one- or two-way ANOVA using GraphPad (PRISM software). Bartlett's tests were used to establish the homogeneity of variance on the basis of the differences among standard deviations. Differences between experimental groups were determined by the Dunnett's test. A value of $P < 0.05$ was considered to be significant.

RESULTS

To investigate the role of endogenous ANP and the NO/cGMP/PKG-Iα signaling pathway in regulating BMSC survival and proliferation, inhibitors and activators of the signaling pathway as well as gene knockdown, utilizing siRNA, were used in the present study, as illustrated in Figure 1.

OP9 CELLS PREDOMINANTLY EXPRESS THE PKG-Iα ISOFORM AND EXPRESS ENDOGENOUS eNOS AND KLF4

Both PKG-Iα (~76 kDa) and PKG-Iβ (~78 kDa) are highly expressed in freshly isolated aorta, as showed by our recent study [Wong and Fiscus, 2010], and another report [Geiselhoringer et al., 2004] on PKG isoforms in mouse tissues. Figure 2A of the present study shows that OP9 cells express predominantly the PKG-Iα isoform. Freshly isolated mouse aorta was used as a positive control. BMSCs also express eNOS and have basal eNOS phosphorylation at serine 1,177, suggesting that endogenous eNOS in BMSCs may provide endogenous NO for downstream activation of the sGC/cGMP/PKG-Iαsignaling pathway for protection against spontaneous apoptosis. BMSCs also express the Kruppel-like factor 4 (KLF4), necessary for survival and proliferation of stem cells, which has previously been shown to bind to the Sp1 promoter of the PKG-Iα gene for regulation of PKG-Iα expression in VSMCs [Zeng et al., 2006].

THE ANP AUTOCRINE LOOP FOR BOTH PROTECTION AGAINST SPONTANEOUS APOPTOSIS AS WELL AS STIMULATION OF CELL PROLIFERATION

Figure 2A shows that OP9 BMSCs express both ANP and the ANP receptor NPR-A, and Figure 2B shows the effects on apoptotic levels of blocking the NPR-A receptors on the surface of BMSCs with the specific ANP antagonist, A71915, which caused significantly higher levels of spontaneous apoptosis. A71915, when used in combination with sGC inhibitor ODQ (which blocks the cytoprotective effects contributed by endogenous NO), causes an even larger increase in apoptosis. Blocking the NPR-A receptors also significantly inhibits proliferation and DNA synthesis (Fig. 2C,D). The data suggest that BMSCs endogenously produce the natriuretic peptide ANP, which in turn causes downstream activation of the cGMP/PKG-Iα pathway. BMSCs may utilize the

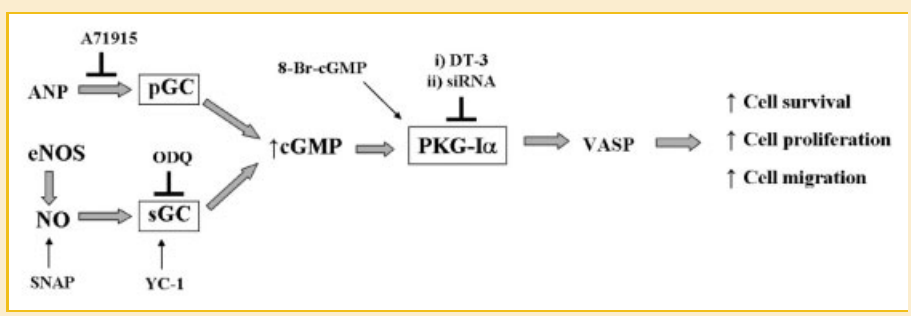

Fig. 1. The NO/sGC/cGMP/PKG-Iα and ANP/pGC(NPR-A)/cGMP/PKG-Iαsignaling pathway are shown, along with the inhibitors and activators used in the present study.

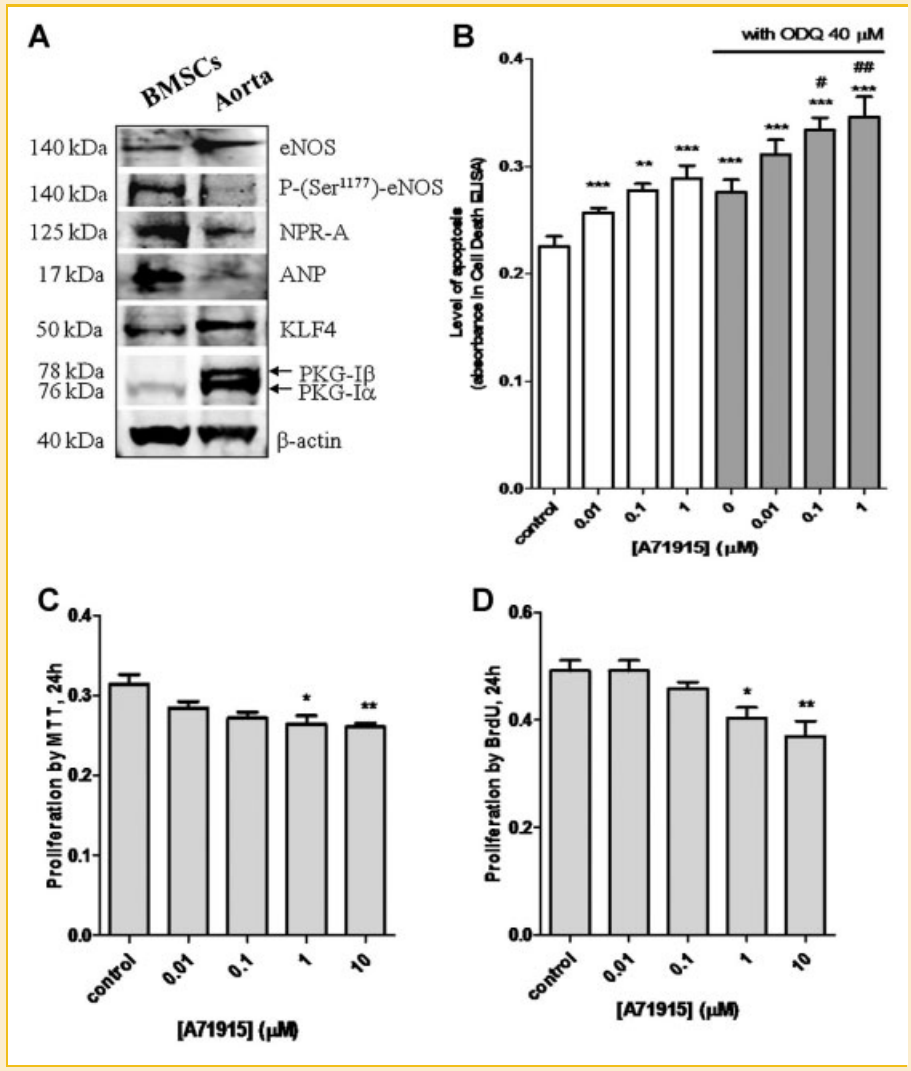

Fig. 2. A: Western blot analysis of the expression of eNOS, phosphorylation of eNOS at Ser-1177, and the expression of NPR-A, ANP precursor, KLF4, and PKG-Iα and PKG-Iβ in OP9 BMSCs and freshly isolated mouse aorta. Total protein (60 μg) was loaded for BMSCs and 20 μg of total protein for the aorta. β-actin was used for normalization. B: Effects on apoptotic levels of blocking the NPR-A receptors with the ANP antagonist A71915 and in combinations with ODQ. *Treatment groups compared with control ($^{*}P<0.05$, $^{**}P<0.01$, $^{***}P<0.001$). #Treatment groups of A71915 used with ODQ compared to the corresponding concentration of A71915 without ODQ ($^{\#}P<0.05$, $^{\#\#}P<0.01$). C and D: Effects on proliferation and DNA synthesis observed from blocking the NPR-A receptors with A71915. Proliferation rates of BMSCs were significantly decreased by A71915 at 1 μM ($^{*}P<0.05$) and 10 μM ($^{**}P<0.01$). The data represent the mean ± SEM of four observations per treatment group.

ANP autocrine loop for both protection against spontaneous apoptosis as well as stimulation of cell proliferation.

BASAL NO/cGMP LEVELS PROTECT BMSCs AGAINST SPONTANEOUS APOPTOSIS

Figure 3A–C shows the effects of a soluble guanylyl cyclase (sGC) inhibitor, ODQ, the NO donor SNAP and the sGC activator YC-1 on the levels of cGMP in OP9 cells. Figure 3D shows a biphasic apoptotic curve in response to increasing concentrations of SNAP. ODQ causes concentration-dependent depletion of basal cGMP levels (Fig. 3A) and apoptosis (Fig. 3D). SNAP is known to release NO at a slow rate, generating NO at a concentration at 0.1% [Crow and Beckman, 1995] to 0.3% [Hirota et al., 2001] of the original SNAP concentration. SNAP at 10 and 50 μM generate NO at 10–50 nM (physiological levels), significantly decreasing the levels of apoptosis, whereas SNAP at 500 and 1,000 μM would generate NO at pathological levels, significantly increasing the levels of apoptosis. YC-1, a sGC activator, at 10 μM to 40 μM, causes ~1.5- to 2-fold increases in cGMP levels and significantly protects BMSCs against spontaneous apoptosis (Fig. 3E). Figure 3F shows ODQ-induced inhibition of endogenous NO-stimulated sGC activity lowers endogenous PKG kinase activity, indicated by Ser239 phosphorylation of VASP. The level of VASP-serine239 phosphorylation was known to be a representation of intracellular PKG activity. Cleaved PARP indicated apoptosis, which confirmed the results from Cell Death ELISA. The data suggest that the basal activation of the NO/cGMP/PKG-Iα signaling pathway in BMSCs is important for protecting against spontaneous onset of apoptosis.

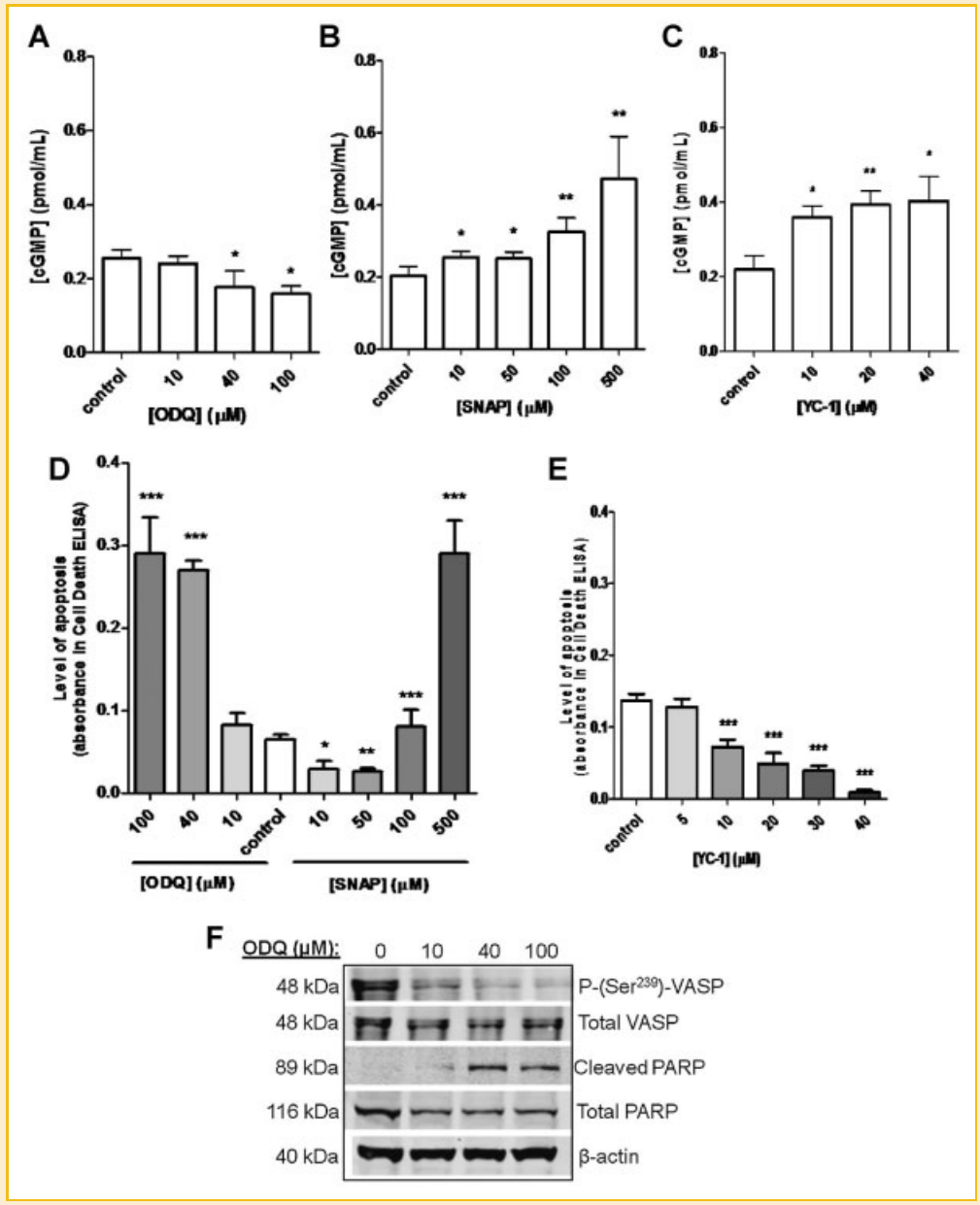

Fig. 3. A: ODQ significantly decreased cGMP levels at 40 and 100 μM ($^{*}P < 0.05$) in BMSCs. B and C: SNAP and YC-1 significantly elevated cGMP levels in BMSCs in a concentration-dependent manner. D: Biphasic apoptotic curve in BMSCs treated with ODQ and SNAP. ODQ, a sGC inhibitor, depleted basal cGMP levels and caused apoptosis at 40 μM ($^{***}P < 0.001$) and 100 μM ($^{***}P < 0.001$), respectively. SNAP, a NO donor, protected cells from apoptosis at 10 μM ($^{*}P < 0.05$) and 50 μM ($^{**}P < 0.01$) and caused apoptosis at 500 μM ($^{***}P < 0.001$). E: YC-1, a sGC activator, protects cells from apoptosis dose dependently from 10 μM to 40 μM ($^{***}P < 0.001$). The data represent the mean ± SEM of six observations per treatment group. F: Western blot analysis showing decreased VASP-phosphorylation at serine239 and increased PARP cleavage in BMSCs treated with ODQ. $^{*}P < 0.05$, $^{**}P < 0.01$, $^{***}P < 0.001$.

These results are consistent with our data in VSMCs [Wong and Fiscus, 2010].

BASAL cGMP LEVELS STIMULATE CELL PROLIFERATION/COLONY FORMATION/MIGRATION

Figure 4A shows that depletion of cGMP by the sGC inhibitor ODQ decreased cell proliferation in MTT assay at 10, 40, 100 μM ($^{***}P < 0.001$). ODQ also inhibits cell migration (Fig. 4C) and colony formation (Fig. 4E,G), suggesting that endogenous PKG-Iα kinase activity (Ser239 phosphorylation of VASP) may play a role in cell migration. The sGC activator YC-1 also inhibited cell proliferation (Fig. 4B), migration (Fig. 4D), and colony formation (Fig. 4F,H), likely via effects unrelated to cGMP (see Discussion).

PRETREATMENT WITH ANP OR 8-Br-cGMP, WHICH BYPASS THE ODQ BLOCK, REVERSES THE ODQ-INDUCED INCREASE IN APOPTOSIS IN BMSCs

The role of PKG-Iα as an important part of the anti-apoptotic/cytoprotective mechanism was confirmed by Figure 5A, showing

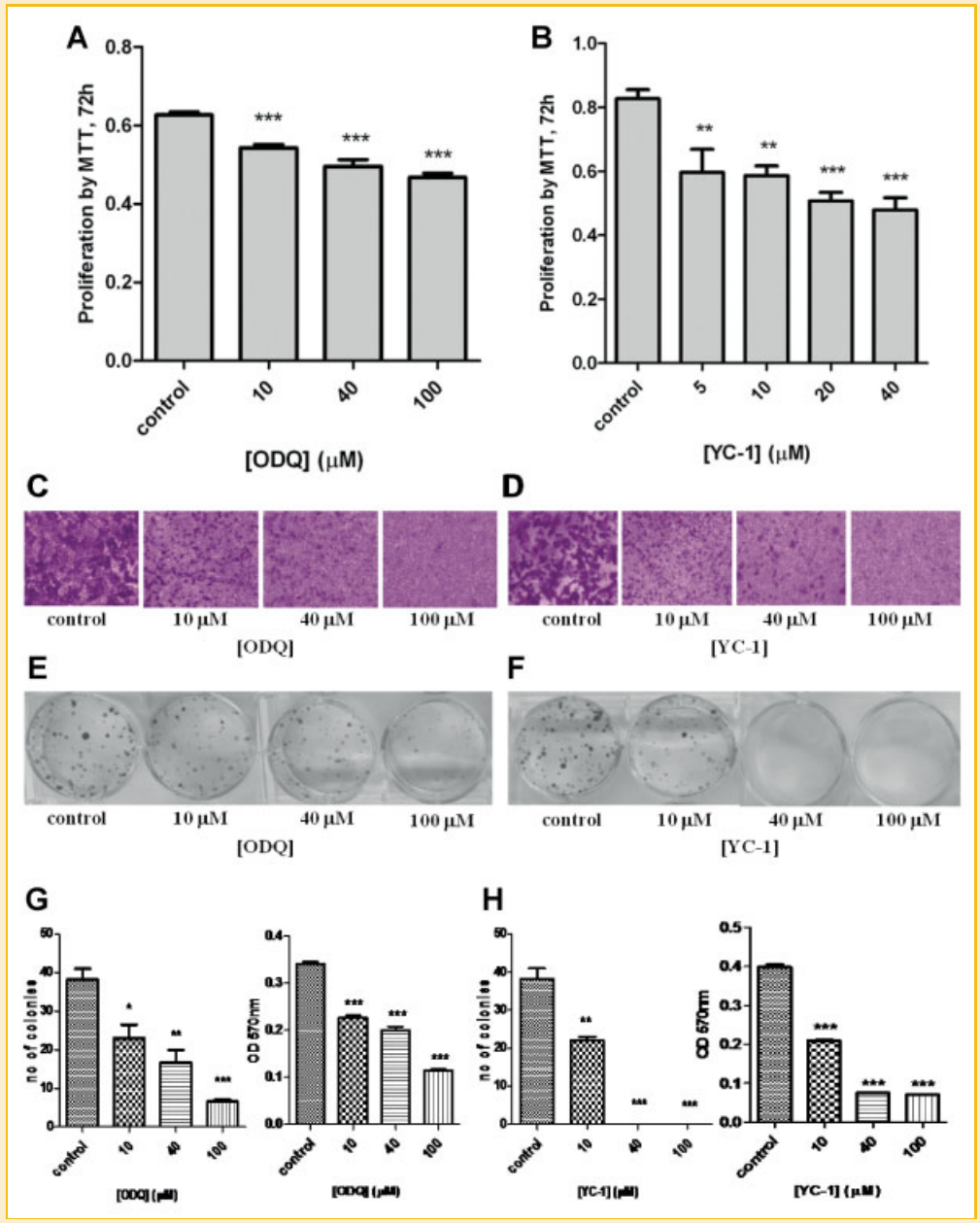

Fig. 4. Cell proliferation, migration, and colony formation were decreased in BMSCs by ODQ and YC-1. A: ODQ inhibits cell proliferation in MTT assay at 10 μM ($^{***}P < 0.001$), 40 μM ($^{***}P < 0.001$), and 100 μM ($^{***}P < 0.001$). B: YC-1 inhibits cell proliferation in MTT assay at 5 μM ($^{**}P < 0.01$), 10 μM ($^{**}P < 0.01$), 20 μM ($^{***}P < 0.001$), and 40 μM ($^{***}P < 0.001$). C and D: Pictures of the cells that have migrated to the bottom of transwell inserts, using staining with crystal violet. The data show inhibition of cell migration by treatment with ODQ and YC-1. E and F: Pictures of colonies formed in six-well plates follows the staining with crystal violet. G and H: Left panel, number of colonies counted (only colonies larger than 500 cells were counted); Right panel, quantification of the crystal violet dye dissolved with 10% acetic acid at 570 nm. The data represent the mean ± SEM of eight observations per treatment group. $^{*}P < 0.05$, $^{**}P < 0.01$, $^{***}P < 0.001$.

that simultaneous addition by 8-bromo-cGMP, a cell-permeable direct activator of PKG-Iα, could almost completely reverse the pro-apoptotic effects of ODQ. Figure 5B shows that exposure of the BMSCs to the natriuretic peptide ANP also causes nearly complete reversal of the ODQ-induced apoptosis. The data further confirm that ANP-induced activation of the NPR-A/cGMP/PKG-Iα signaling pathway can protect (almost completely) the BMSCs from the pro-apoptotic effects of ODQ. The data suggest that BMSCs utilize both sGC, which is stimulated by endogenously-produced NO, and NPR-A (a particulate guanylyl cyclase), which is stimulated by endogenously-produced ANP, to protect against spontaneous onset of apoptosis.

BASAL PKG-Iα ACTIVITY IN BMSCs PROTECTS AGAINST INDUCTION OF APOPTOSIS

To further investigate the anti-apoptotic role of PKG-Iα in BMSCs, a specific PKG-Iαinhibitor, DT-3, was used. DT-3 can effectively inhibit not only stimulated PKG activity, but also basal PKG activity

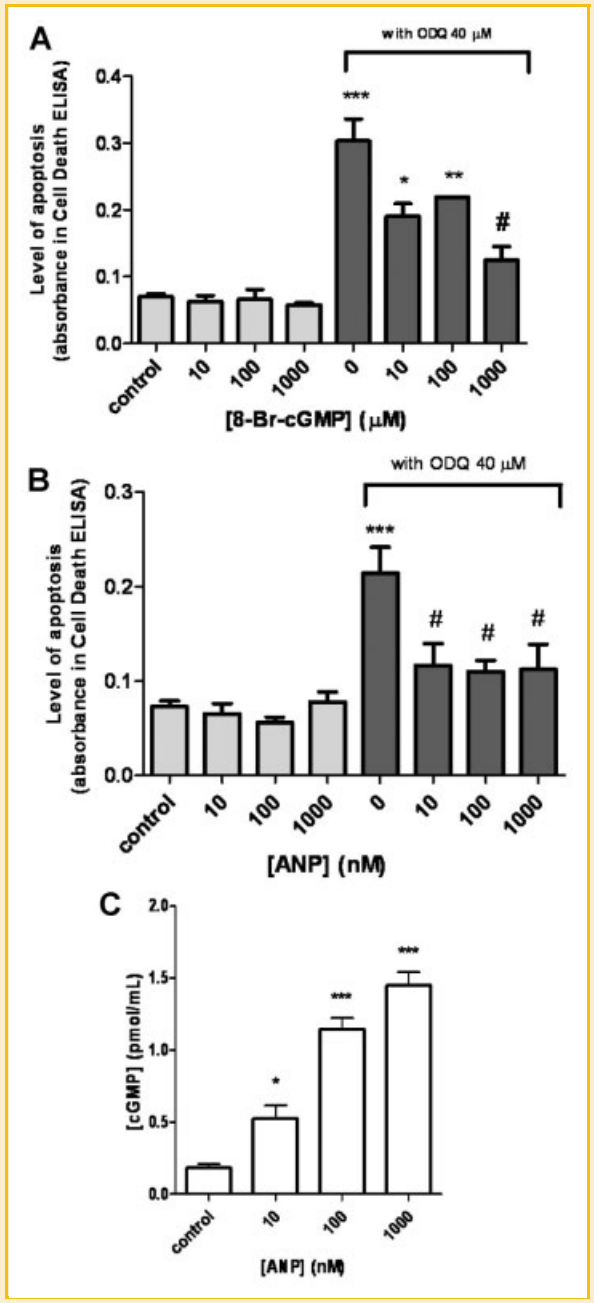

Fig. 5. A: 8-Br-cGMP reverses the ODQ-induced increase in apoptosis in BMSCs. 8-Br-cGMP, at 1,000 μM ($^{\#}P < 0.05$), a direct activator of PKG, prevented apoptosis caused by depletion of cGMP by ODQ (40 μM). B: ANP completely abolished the ODQ-induced apoptosis in BMSCs. ANP at 10 nM ($^{\#}P < 0.05$), 100 nM ($^{\#}P < 0.05$) and 1,000 nM ($^{\#}P < 0.05$), a particulate guanylyl cyclase activator, completely prevented ODQ-induced apoptosis. C: ANP elevated cGMP levels in BMSCs in a concentration-dependent manner. The data represent the mean ± SEM of four observations per treatment group. *Treatment groups compared with control ($^{*}P < 0.05$, $^{**}P < 0.01$, $^{***}P < 0.001$). #Treatment groups compared with ODQ (40 μM) alone.

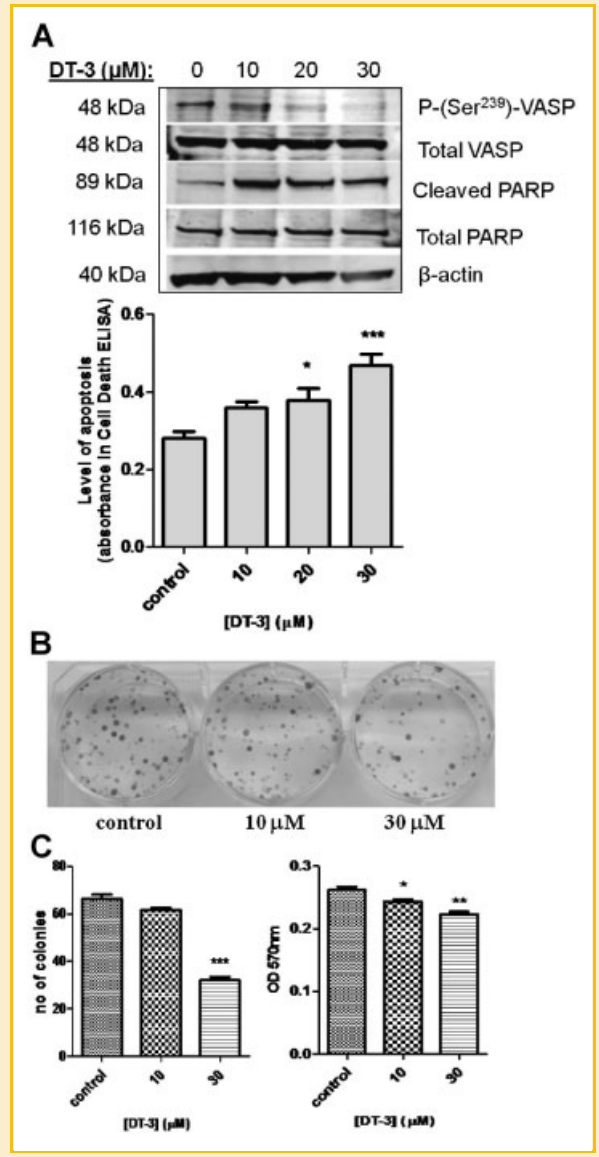

Fig. 6. Inhibition of endogenous PKG activity caused induction of apoptosis, inhibition of cell proliferation and colony formation in BMSCs. A: Upper panel, Western blot analysis showing decreased VASP-phosphorylation at serine239 and increased PARP cleavage in BMSCs treated with DT-3, a PKG-Iα inhibitor; Lower panel, DT-3 significantly induced apoptosis (determined by Cell Death Detection ELISA) at 20 μM ($^{*}P < 0.05$) and 30 μM ($^{***}P < 0.001$). B: Pictures showing DT-3 decreased colony formation in BMSCs. C, Left, number of colonies counted (only colonies larger than 500 cells were counted); Right, quantification of the crystal violet dye dissolved with 10% acetic acid at 570 nm. The data represent the mean ± SEM of four observations per treatment group. $^{*}P < 0.05$, $^{**}P < 0.01$, $^{***}P < 0.001$.

[Dostmann et al., 2002; Taylor et al., 2004]. Western blot analysis in Figure 6 shows DT-3 effectively decreased VASP-phosphorylation at serine239, an indication of intracellular PKG kinase activity. DT-3 also significantly induced apoptosis at 20 μM ($^{*}P < 0.05$) and 30 μM ($^{***}P < 0.001$), apoptosis results confirmed by increased PARP cleavage (Fig. 6A). PKG-Iα-siRNA at 100 nM increased apoptosis (Fig. 7B). Apoptosis results were confirmed by increased PARP cleavage (Fig. 7D). PKG-Iα-siRNA at 50 nM and 100 nM cause approximately 40% and 60% knockdown of PKG expression, as shown by Western blot analysis (Fig. 7C). PKG-Iα-siRNA at 50 nM and 100 nM both effectively decreased intracellular PKG kinase activity (VASP-phosphorylation at serine239) (Fig. 7D).

BASAL PKG ACTIVITY IN BMSCs STIMULATES CELL PROLIFERATION, COLONY FORMATION, AND CELL MIGRATION

Figure 6B,C show that DT-3 decreased colony formation in BMSCs. The result is further confirmed by PKG-Iα knockdown in Figure 7A. PKG-Iα-siRNA at 50 nM and 100 nM also decreased cell migration (Fig. 7E). PKG-Iα knockdown with PKG-Iα-siRNA (100 nM) decreased de novo DNA synthesis (Fig. 7F) and proliferation (Fig. 7G) at 24, 48, and 72 h, respectively. The data suggest that basal PKG activity in BMSCs is essential for stimulating cell proliferation and cell migration.

DISCUSSION

BMSCs are adherent, fibroblast-like cells in the adult bone marrow [Friedenstein et al., 1968]. BMSCs are multipotent stem cells, and are capable of differentiating along the mesenchymal lineage to form bone, fat, and cartilage. Hence, over recent years, the potential for the use of BMSCs in stem cell therapy for replacing damaged bone, cartilage, and muscle, especially, for example, cardiac muscle after heart attack, have been implicated [Psaltis et al., 2008]. The BMSC line OP9 has been used in coculture systems as a feeder layer with mouse ES cells and iPS cells to induce the differentiation of ES cells and iPS cells along hematopoietic lineages [Nakano et al., 1994; Nakano, 1995; Kitajima et al., 2003; Ji et al., 2008]. OP9 cells can also be differentiated into adipocytes and used as a model for adipogenesis [Wolins et al., 2006].

Our early studies were the first to show that NO, both therapeutically-administered NO and endogenous endothelium-derived NO, stimulates the intracellular activity of PKG in VSMCs [Fiscus et al., 1983], and that ANP stimulates intracellular PKG in VSMCs [Fiscus et al., 1985]. These studies led to later establishment of PKG as the key protein kinase mediating the biological effects (e.g., vasodilation and anti-hypertensive effects) of NO and the natriuretic peptides [Fiscus, 1988, 2002; Fiscus and Murad, 1988; Lincoln et al., 2001; Fung et al., 2005]. Recently, our laboratory has shown that many mammalian cells, including epithelial cells, neural cells, and various cancer cells (e.g., breast cancer, lung cancer, mesothelioma, ovarian cancer, prostate cancer, and VSMCs), all express at least one or both of the two PKG-I isoforms, PKG-Iα and PKG-Iβ, and that the PKG-Iα isoform is essential for the survival and proliferation of these cells [Fiscus et al., 2001, 2002; Fiscus, 2002; Chan and Fiscus, 2003; Cheng Chew et al., 2003; Fung et al., 2005; Fraser et al., 2006; Leung et al., 2008, 2010; Johlfs and Fiscus, 2010; Wong and Fiscus, 2010].

The present study shows that phosphorylation of VASP at serine 239 serves as a useful indicator of endogenous PKG activity in the BMSCs. VASP is a PKG downstream substrate that is directly phosphorylated at Ser239 by PKG in a number of mammalian cells [Butt et al., 1994; Chen et al., 2008; Isenberg et al., 2008], but the present study shows PKG-mediated phosphorylation of VASP in BMSCs for the first time. VASP is an actin-binding protein involved in focal adhesion [Butt et al., 1994], and VASP phosphorylation at ser239 by PKG was shown to cause redistribution of VASP to the plasma membrane, and thereby may promote cell attachment and migration, potentially also promoting cell survival and proliferation [Harbeck et al., 2000; Li Calzi et al., 2008].

Human BMSCs have been reported to synthesize and release endogenous brain (B-type) natriuretic peptide (BNP) and the released BNP was proposed to mediate the neuroprotective effects of BMSCs in animal model of stroke [Song et al., 2004]. The present study using OP9 BMSCs shows that these cells produce detectable levels of ANP precursor [Noyan-Ashraf et al., 2009] (Fig. 2A), suggesting that these cells likely synthesize and release ANP, similar to the data of a previous study showing endogenous production of another natriuretic peptide, BNP, in human BMSCs [Song et al., 2004], and that released ANP activates the NPR-A receptors to stimulate cell proliferation and survival of the OP9 cells. This mechanism may provide an autocrine loop that protects BMSCs from spontaneous apoptosis and stimulates cell proliferation.

The present study suggests that basal activation of the NO/cGMP/PKG-Iα signaling pathway in BMSCs is important for cell proliferation, colony formation and migration. However, the sGC activator YC-1 also inhibited cell proliferation (Fig. 4B), migration (Fig. 4D), and colony formation (Fig. 4F,H). These anti-proliferative, anti-colony formation, and anti-migration effects are likely to be mediated by other effects of YC-1 (which are independent of cGMP) [Pan et al., 2005]. In another example, YC-1 has been shown to have anti-proliferative effects in hepatocellular carcinoma cells by a mechanism that is independent of its effects on the cGMP signaling pathway and instead involves YC-1-induced up-regulation of $p21^{CIP1/wap1}$ [Wang et al., 2005].

Figure 8 shows a cellular model illustrating the findings of the present study. Also included in the model are the phosphorylation of other downstream target proteins, BAD [Johlfs and Fiscus, 2010], CREB [Fiscus, 2002], and Src [Leung et al., 2010], previously reported by our laboratory as intracellular proteins that are directly phosphorylated by PKG-Iα promoting cell proliferation and survival. The data from the present study suggest that BMSCs utilize both the NO/sGC/cGMP/PKG-Iα pathway and the ANP/NPR-A/cGMP/PKG-Iα pathway, in an autocrine loop fashion, to protect the cells from spontaneous onset of apoptosis and to stimulate cell proliferation. Furthermore, the present study shows that these signaling pathways promote migration of the OP9 BMSCs, shown in the model of Figure 8. In the bone marrow micro-environmental niche, endothelial cells, which are in close proximity to BMSCs,

Fig. 7. Gene knockdown of PKG-Iα expression using PKG-Iα-siRNA increased apoptosis and decreased proliferation in BMSCs. A: PKG-Iα knockdown decreased BMSC colony formation. B: Gene knockdown by PKG-Iα-siRNA (100 nM) significantly ($^{**}P < 0.01$) increased spontaneous apoptosis compared to negative control. C: Western blot analysis showing decreased PKG-Iα expression after treatment with PKG-Iα-siRNA. The relative intensity of the bands in the western blots were quantified, showing about 40% and 60% knockdown at 50 nM and 100 nM, respectively. D: Western blot analysis showing decreased VASP-phosphorylation at serine239 and increased PARP cleavage in BMSCs after gene knockdown of PKG-Iα. E: PKG-Iα knockdown decreased cell migration. F and G, PKG-Iα knockdown decreased de novo DNA synthesis at 48 h ($^{*}P < 0.05$) and 72 h ($^{**}P < 0.01$) in cultures treated with PKG-Iα-siRNA (100 nM). Similar results obtained by MTT assay. PKG-Iα knockdown decreased proliferation at 24 h ($^{***}P < 0.001$), 48 h ($^{***}P < 0.001$), and 72 h ($^{***}P < 0.001$). The data represent the mean ± SEM of six observations per treatment group.

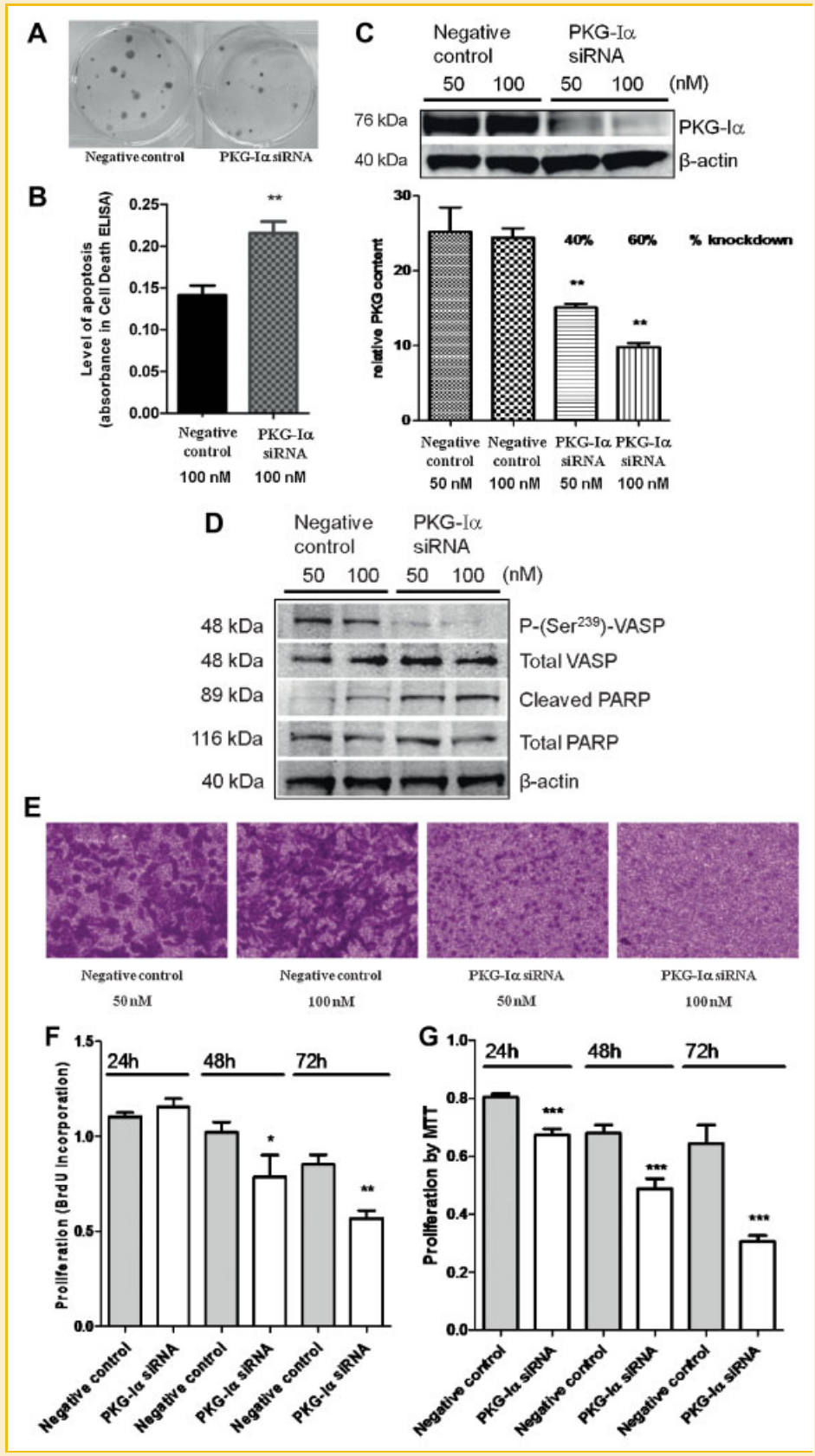
A
Negative control
PKG-Iα siRNA
B
Level of apoptosis (absorbance in Cell Death ELISA)
0.25
0.20
0.15
0.10
0.05
0.00
**
Negative control
PKG-Iα siRNA
100 nM
100 nM
C
Negative control
PKG-Iα siRNA
50
100
50
100
(nM)
76 kDa
40 kDa
PKG-Iα
β-actin
relative PKG content
30
20
10
0
40%
60%
% knockdown
**
**
Negative control
Negative control
PKG-Iα siRNA
PKG-Iα siRNA
50 nM
100 nM
50 nM
100 nM
D
Negative control
PKG-Iα siRNA
50
100
50
100
(nM)
48 kDa
48 kDa
89 kDa
116 kDa
40 kDa
P-(Ser239)-VASP
Total VASP
Cleaved PARP
Total PARP
β-actin
E
Negative control
50 nM
Negative control
100 nM
PKG-Iα siRNA
50 nM
PKG-Iα siRNA
100 nM
F
Proliferation (BrdU incorporation)
1.5
1.0
0.5
0.0
24h
48h
72h
*
**
Negative control
PKG-Iα siRNA
Negative control
PKG-Iα siRNA
Negative control
PKG-Iα siRNA
G
Proliferation by MTT
1.0
0.8
0.6
0.4
0.2
0.0
24h
48h
72h
***
***
***
Negative control
PKG-Iα siRNA
Negative control
PKG-Iα siRNA
Negative control
PKG-Iα siRNA

Fig. 7.

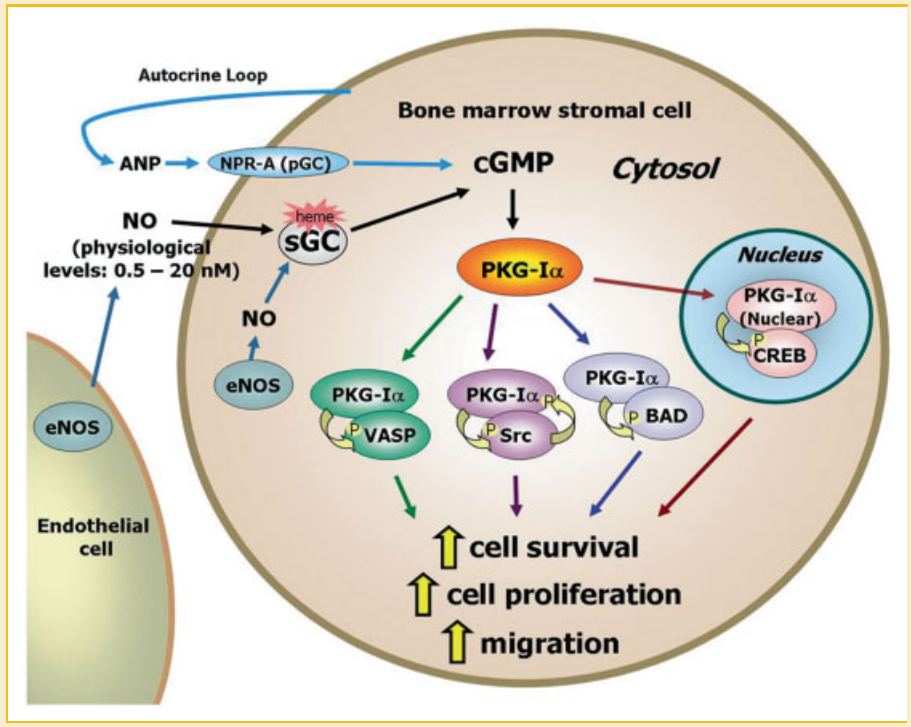

Fig. 8. The overall model illustrating the findings of the present study. BMSCs utilize the NO/sGC/cGMP/PKG-Iα signaling pathway as well as the ANP/pGC(NPR-A)/cGMP/PKG-Iα signaling pathway to stimulate cell proliferation and inhibit spontaneous onset of apoptosis. ANP released from BMSCs may participate in a novel autocrine loop mechanism for regulating BMSC survival and proliferation. Also, natriuretic peptides and NO, released from nearby endothelial cells in the bone marrow stroma, may also participate as a paracrine mechanism regulating BMSC survival and proliferation.

provide another source of endogenous NO. Also, endothelial cells are reported to synthesize and release all three natriuretic peptides, ANP, BNP, and CNP [Bordenave et al., 2002], which may also potentially stimulate BMSC survival and proliferation via a paracrine mechanism. Therefore, the cytoprotective and growth-promoting mechanism involving the NO/sGC/cGMP/PKG-Iα and ANP/NPR-A/cGMP/PKG-Iα pathways may play an important role within the bone marrow to provide a healthy micro-environmental niche for the survival, growth, and differentiation of HSCs. Furthermore, the data of the present study provide a unique insight into a key cell signaling pathway in OP9 cells that could be used to develop new strategies for improving ex vivo survival and expansion of these cells or similar cells.

REFERENCES

Bordenave L, Georges A, Bareille R, Conrad V, Villars F, Amedee J. 2002. Human bone marrow endothelial cells: A new identified source of B-type natriuretic peptide. Peptides 23:935–940.

Butt E, Abel K, Krieger M, Palm D, Hoppe V, Hoppe J, Walter U. 1994. cAMP- and cGMP-dependent protein kinase phosphorylation sites of the focal adhesion vasodilator-stimulated phosphoprotein (VASP) in vitro and in intact human platelets. J Biol Chem 269:14509–14517.

Caplan AI. 1991. Mesenchymal stem cells. J Orthop Res 9:641–650.

Chan SL, Fiscus RR. 2003. Guanylyl cyclase inhibitors NS2028 and ODQ and protein kinase G (PKG) inhibitor KT5823 trigger apoptotic DNA fragmentation in immortalized uterine epithelial cells: Anti-apoptotic effects of basal cGMP/PKG. Mol Hum Reprod 9:775–783.

Charles N, Ozawa T, Squatrito M, Bleau AM, Brennan CW, Hambardzumyan D, Holland EC. 2010. Perivascular nitric oxide activates notch signaling and promotes stem-like character in PDGF-induced glioma cells. Cell Stem Cell 6:141–152.

Chen H, Levine YC, Golan DE, Michel T, Lin AJ. 2008. Atrial natriuretic peptide-initiated cGMP pathways regulate vasodilator-stimulated phosphoprotein phosphorylation and angiogenesis in vascular endothelium. J Biol Chem 283:4439–4447.

Cheng Chew SB, Leung PY, Fiscus RR. 2003. Preincubation with atrial natriuretic peptide protects NG 108–15 cells against the toxic/proapoptotic effects of the nitric oxide donor S-nitroso- N-acetylpenicillamine. Histochem Cell Biol 120:163–171.

Crow JP, Beckman JS. 1995. Reactions between nitric oxide, superoxide, and peroxynitrite: Footprints of peroxynitrite in vivo. Adv Pharmacol 34:17–43.

Dostmann WR, Tegge W, Frank R, Nickl CK, Taylor MS, Brayden JE. 2002. Exploring the mechanisms of vascular smooth muscle tone with highly specific, membrane-permeable inhibitors of cyclic GMP-dependent protein kinase Ialpha. Pharmacol Ther 93:203–215.

Fiscus RR. 1988. Molecular mechanisms of endothelium-mediated vasodilation. Semin Thromb Hemost 14(Suppl.):12–22.

Fiscus RR. 2002. Involvement of cyclic GMP and protein kinase G in the regulation of apoptosis and survival in neural cells. Neurosignals 11:175–190.

Fiscus RR, Murad F. 1988. cGMP-dependent protein kinase activation in intact tissues. Methods Enzymol 159:150–159.

Fiscus RR, Rapoport RM, Murad F. 1983. Endothelium-dependent and nitrovasodilator-induced activation of cyclic GMP-dependent protein kinase in rat aorta. J Cyclic Nucleotide Protein Phosphor Res 9:415–425.

Fiscus RR, Rapoport RM, Waldman SA, Murad F. 1985. Atriopeptin II elevates cyclic GMP, activates cyclic GMP-dependent protein kinase and causes relaxation in rat thoracic aorta. Biochim Biophys Acta 846:179–184.

Fiscus RR, Tu AW, Chew SB. 2001. Natriuretic peptides inhibit apoptosis and prolong the survival of serum-deprived PC12 cells. Neuroreport 12:185–189.

Fiscus RR, Yuen JP, Chan SL, Kwong JH, Chew SB. 2002. Nitric oxide and cyclic GMP as pro- and anti-apoptotic agents. J Card Surg 17:336–339.

Fraser M, Chan SL, Chan SS, Fiscus RR, Tsang BK. 2006. Regulation of p53 and suppression of apoptosis by the soluble guanylyl cyclase/cGMP pathway in human ovarian cancer cells. Oncogene 25:2203–2212.

Friedenstein AJ, Petrakova KV, Kurolesova AI, Frolova GP. 1968. Heterotopic of bone marrow. Analysis of precursor cells for osteogenic and hematopoietic tissues. Transplantation 6:230–247.

Fung E, Fiscus RR, Yim AP, Angelini GD, Arifi AA. 2005. The potential use of type-5 phosphodiesterase inhibitors in coronary artery bypass graft surgery. Chest 128:3065–3073.

Geiselhoringer A, Gaisa M, Hofmann F, Schlossmann J. 2004. Distribution of IRAG and cGKI-isoforms in murine tissues. FEBS Lett 575:19–22.

Harbeck B, Huttelmaier S, Schluter K, Jockusch BM, Illenberger S. 2000. Phosphorylation of the vasodilator-stimulated phosphoprotein regulates its interaction with actin. J Biol Chem 275:30817–30825.

Hassan HT, El-Sheemy M. 2004. Adult bone-marrow stem cells and their potential in medicine. J R Soc Med 97:465–471.

Hirota Y, Ishida H, Genka C, Obama R, Matsuyama S, Nakazawa H. 2001. Physiological concentration of nitric oxide induces positive inotropic effects through cGMP pathway in isolated rat ventricular myocytes. Jpn J Physiol 51:455–461.

Isenberg JS, Romeo MJ, Yu C, Yu CK, Nghiem K, Monsale J, Rick ME, Wink DA, Frazier WA, Roberts DD. 2008. Thrombospondin-1 stimulates platelet aggregation by blocking the antithrombotic activity of nitric oxide/cGMP signaling. Blood 111:613–623.

Ji J, Vijayaragavan K, Bosse M, Menendez P, Weisel K, Bhatia M. 2008. OP9 stroma augments survival of hematopoietic precursors and progenitors during hematopoietic differentiation from human embryonic stem cells. Stem Cells 26:2485–2495.

Johlfs MG, Fiscus RR. 2010. Protein kinase G type-Ialpha phosphorylates the apoptosis-regulating protein Bad at serine 155 and protects against apoptosis in N1E-115 cells. Neurochem Int 56:546–553.

Kelly MA, Hirschi KK. 2009. Signaling hierarchy regulating human endothelial cell development. Arterioscler Thromb Vasc Biol 29:718–724.

Kitada M, Dezawa M. 2009. Induction system of neural and muscle lineage cells from bone marrow stromal cells; a new strategy for tissue reconstruction in degenerative diseases. Histol Histopathol 24:631–642.

Kitajima K, Tanaka M, Zheng J, Sakai-Ogawa E, Nakano T. 2003. In vitro differentiation of mouse embryonic stem cells to hematopoietic cells on an OP9 stromal cell monolayer. Methods Enzymol 365:72–83.

Krumenacker JS, Murad F. 2006. NO-cGMP signaling in development and stem cells. Mol Genet Metab 87:311–314.

Krumenacker JS, Katsuki S, Kots A, Murad F. 2006. Differential expression of genes involved in cGMP-dependent nitric oxide signaling in murine embryonic stem (ES) cells and ES cell-derived cardiomyocytes. Nitric Oxide 14:1–11.

Leung EL, Fraser M, Fiscus RR, Tsang BK. 2008. Cisplatin alters nitric oxide synthase levels in human ovarian cancer cells: Involvement in p53 regulation and cisplatin resistance. Br J Cancer 98:1803–1809.

Leung EL, Wong JC, Johlfs MG, Tsang BK, Fiscus RR. 2010. Protein kinase G type Ialpha activity in human ovarian cancer cells significantly contributes to enhanced Src activation and DNA synthesis/cell proliferation. Mol Cancer Res 8:578–591.

Li Calzi S, Purich DL, Chang KH, Afzal A, Nakagawa T, Busik JV, Agarwal A, Segal MS, Grant MB. 2008. Carbon monoxide and nitric oxide mediate cytoskeletal reorganization in microvascular cells via vasodilator-stimulated phosphoprotein phosphorylation: Evidence for blunted responsiveness in diabetes. Diabetes 57:2488–2494.

Lincoln TM, Dey N, Sellak H. 2001. Invited review: cGMP-dependent protein kinase signaling mechanisms in smooth muscle: From the regulation of tone to gene expression. J Appl Physiol 91:1421–1430.

Nakano T. 1995. Lymphohematopoietic development from embryonic stem cells in vitro. Semin Immunol 7:197–203.

Nakano T, Kodama H, Honjo T. 1994. Generation of lymphohematopoietic cells from embryonic stem cells in culture. Science 265:1098–1101.

Niwa A, Umeda K, Chang H, Saito M, Okita K, Takahashi K, Nakagawa M, Yamanaka S, Nakahata T, Heike T. 2009. Orderly hematopoietic development of induced pluripotent stem cells via Flk-1(+) hemoangiogenic progenitors. J Cell Physiol 221:367–377.

Noyan-Ashraf MH, Momen MA, Ban K, Sadi AM, Zhou YQ, Riazi AM, Baggio LL, Henkelman RM, Husain M, Drucker DJ. 2009. GLP-1R agonist liraglutide activates cytoprotective pathways and improves outcomes after experimental myocardial infarction in mice. Diabetes 58:975–983.

Pan SL, Guh JH, Peng CY, Wang SW, Chang YL, Cheng FC, Chang JH, Kuo SC, Lee FY, Teng CM. 2005. YC-1 [3-(5'-hydroxymethyl-2'-furyl)-1-benzyl indazole] inhibits endothelial cell functions induced by angiogenic factors in vitro and angiogenesis in vivo models. J Pharmacol Exp Ther 314:35–42.

Psaltis PJ, Zannettino AC, Worthley SG, Gronthos S. 2008. Concise review: Mesenchymal stromal cells: Potential for cardiovascular repair. Stem Cells 26:2201–2210.

Sadan O, Melamed E, Offen D. 2009. Bone-marrow-derived mesenchymal stem cell therapy for neurodegenerative diseases. Expert Opin Biol Ther 9:1487–1497.

Song S, Kamath S, Mosquera D, Zigova T, Sanberg P, Vesely DL, Sanchez-Ramos J. 2004. Expression of brain natriuretic peptide by human bone marrow stromal cells. Exp Neurol 185:191–197.

Taylor MS, Okwuchukwuasanya C, Nickl CK, Tegge W, Brayden JE, Dostmann WR. 2004. Inhibition of cGMP-dependent protein kinase by the cell-permeable peptide DT-2 reveals a novel mechanism of vasoregulation. Mol Pharmacol 65:1111–1119.

Wang SW, Pan SL, Guh JH, Chen HL, Huang DM, Chang YL, Kuo SC, Lee FY, Teng CM. 2005. YC-1 [3-(5'-hydroxymethyl-2'-furyl)-1-benzyl Indazole] exhibits a novel antiproliferative effect and arrests the cell cycle in G0-G1 in human hepatocellular carcinoma cells. J Pharmacol Exp Ther 312:917–925.

Wilson A, Trumpp A. 2006. Bone-marrow haematopoietic-stem-cell niches. Nat Rev Immunol 6:93–106.

Wolins NE, Quaynor BK, Skinner JR, Tzekov A, Park C, Choi K, Bickel PE. 2006. OP9 mouse stromal cells rapidly differentiate into adipocytes: Characterization of a useful new model of adipogenesis. J Lipid Res 47:450–460.

Wong JC, Fiscus RR. 2010. Protein kinase G activity prevents pathological-level nitric oxide-induced apoptosis and promotes DNA synthesis/cell proliferation in vascular smooth muscle cells. Cardiovasc Pathol 19:e221–e231.

Zeng Y, Zhuang S, Gloddek J, Tseng CC, Boss GR, Pilz RB. 2006. Regulation of cGMP-dependent protein kinase expression by Rho and Kruppel-like transcription factor-4. J Biol Chem 281:16951–16961.